



**HAL**  
open science

## Comprehensive Insights into the Production of Long Chain Aliphatic Aldehydes Using a Copper-Radical Alcohol Oxidase as Biocatalyst

David Ribeaucourt, Bastien Bissaro, Victor Guallar, Mehdi Yemloul, Mireille Haon, Sacha Grisel, Véronique Alphand, Harry Brumer, Fanny Lambert, Jean-Guy Berrin, et al.

► **To cite this version:**

David Ribeaucourt, Bastien Bissaro, Victor Guallar, Mehdi Yemloul, Mireille Haon, et al.. Comprehensive Insights into the Production of Long Chain Aliphatic Aldehydes Using a Copper-Radical Alcohol Oxidase as Biocatalyst. ACS Sustainable Chemistry & Engineering, 2021, 9 (12), pp.4411-4421. 10.1021/acssuschemeng.0c07406 . hal-03619465

**HAL Id: hal-03619465**

**<https://hal.science/hal-03619465v1>**

Submitted on 3 May 2022

**HAL** is a multi-disciplinary open access archive for the deposit and dissemination of scientific research documents, whether they are published or not. The documents may come from teaching and research institutions in France or abroad, or from public or private research centers.

L'archive ouverte pluridisciplinaire **HAL**, est destinée au dépôt et à la diffusion de documents scientifiques de niveau recherche, publiés ou non, émanant des établissements d'enseignement et de recherche français ou étrangers, des laboratoires publics ou privés.

# Comprehensive insights into the production of long chain aliphatic aldehydes using a copper-radical alcohol oxidase as biocatalyst

*David Ribeaucourt<sup>1,2,3</sup>, Bastien Bissaro<sup>1</sup>, Victor Guallar<sup>4,5</sup>, Mehdi Yemloul<sup>2</sup>, Mireille Haon<sup>1</sup>,  
Sacha Grisel<sup>1</sup>, Véronique Alphand<sup>2</sup>, Harry Brumer<sup>6</sup>, Fanny Lambert<sup>3</sup>, Jean-Guy Berrin<sup>1\*</sup> and  
Mickael Lafond<sup>2\*</sup>*

<sup>1</sup>INRAE, Aix Marseille Univ, UMR1163 Biodiversité et Biotechnologie Fongiques, 13009, Marseille, France

<sup>2</sup> Aix Marseille Univ, CNRS, Centrale Marseille, iSm2, Marseille, France

<sup>3</sup> V. Mane Fils, 620 route de Grasse, 06620 Le Bar sur Loup, France

<sup>4</sup>Joint BSC-CRG-IRB Research Program in Computational Biology, Barcelona Supercomputing Center, Jordi Girona 29, E-08034 Barcelona, Spain

<sup>5</sup>Institució Catalana de Recerca i Estudis Avançats (ICREA), 08010 Barcelona, Spain

<sup>6</sup>Michael Smith Laboratories and Department of Chemistry, University of British Columbia, 2185 East Mall, Vancouver, BC, V6T 1Z4, Canada

\* corresponding authors: Jean-Guy Berrin ([jean-guy.berrin@inrae.fr](mailto:jean-guy.berrin@inrae.fr)) and Mickael Lafond

([mickael.lafond@univ-amu.fr](mailto:mickael.lafond@univ-amu.fr))

## ABSTRACT

1 The oxidation of alcohols is a cornerstone reaction in chemistry, notably in the flavors and  
2 fragrances industry where long chain aliphatic aldehydes are major odorant compounds. In a  
3 context where greener alternatives are sought after, biocatalysis holds many promises. Here, we  
4 investigated the ability of the alcohol oxidase from *Colletotrichum graminicola* (CgrAlcOx) – an  
5 organic cofactor-free enzyme belonging to the copper-radical oxidases (CROs) class – to convert  
6 industrially-relevant long chain aliphatic alcohols. CgrAlcOx is a competent catalyst for the  
7 conversion of octan-1-ol, when supported by the accessory enzymes peroxidase and catalase.  
8 Detailed examination of the products revealed the occurrence of an overoxidation step leading to  
9 the production of carboxylic acid for some aliphatic aldehydes and benzaldehyde derivatives. The  
10 partition between aldehyde and acid products varied upon substrate properties (chain length and  
11 propensity to form *geminal*-diols), enzyme specificity, and could be tuned by controlling the  
12 reaction conditions. *In silico* analyses suggested an inhibitory binding mode of long chain aliphatic  
13 *geminal*-diols and a substrate-induced fit mechanism for a benzyl alcohol-derivative. By  
14 demonstrating their natural ability to perform long chain aliphatic alcohol oxidation, the present  
15 study establishes the potential of fungal CRO-AlcOx as promising candidates for the green  
16 production of flavors and fragrances compounds.

17  
18  
19 **KEYWORDS:** Biocatalysts, Copper-Radical Oxidases, Alcohol-Oxidases, Long Chain Aliphatic  
20 Alcohols, Fragrant Aldehydes.

21  
22  
23

## 24 INTRODUCTION

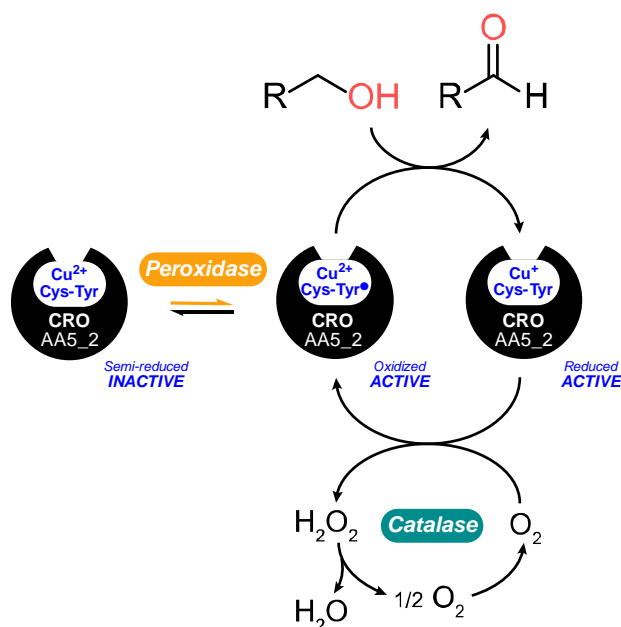
25

26 The oxidation of alcohols to aldehydes is a major reaction in the fine chemical industry<sup>1-3</sup>.  
27 Aldehydes are key intermediates for organic synthesis in applications such as pharmaceuticals or  
28 alkene synthesis<sup>4</sup>, but also valuable final products such as flavors and fragrances ingredients<sup>5-7</sup>.  
29 Traditional chemical processes for the oxidation of alcohols usually entail the use of toxic catalysts  
30 such as chromium VI<sup>8</sup>, hence calling for the development of eco-friendly alternatives. Yet, many  
31 challenges obstruct the different biocatalytic paths that can be envisioned, especially for the water  
32 insoluble and poorly reactive unactivated long chain aliphatic alcohols. Amongst the broad class  
33 of aldehydes, long chain aliphatic aldehydes from C6 to C10<sup>9-12</sup> are of main importance for the  
34 flavor and fragrance industry. Indeed, such aldehydes have been identified as one of the most  
35 prominent classes of “key food odorants”<sup>11</sup>, and are also major fragrance ingredients, used in  
36 quasi-all types of perfumes<sup>6,13</sup>. Typically, long chain aliphatic aldehydes provide green, fruity,  
37 fresh, citrus-like, fatty, or the so-called aldehydic notes<sup>14,15</sup>. Long chain aliphatic aldehydes can be  
38 enzymatically obtained *via* reduction of their acid counterpart using carboxylic acid reductases  
39 (CARs - EC 1.2.1.30). However, CARs are intracellular FAD-dependent enzymes, requiring ATP  
40 supply and NADP/NADPH recycling systems<sup>16</sup>, which renders their use hardly compatible with  
41 industrial constraints. Alternatively, long chain aliphatic aldehydes can be obtained *via* the  
42 oxidation of the corresponding alcohols but only a handful of long chain alcohol oxidoreductases  
43 have hitherto been discovered, characterized and engineered for this purpose<sup>12,17,18</sup>. These  
44 oxidoreductases include NAD(P)<sup>+</sup>-dependent alcohol dehydrogenases (ADHs - EC 1.1.1.1) and  
45 flavin-dependent alcohol oxidases (FAD-AOXs - EC 1.1.3.13)<sup>19</sup>. ADHs are well-established  
46 biocatalysts despite the reversible, unfavorable and nicotinamide-dependent nature of the alcohol

47 oxidation reaction they catalyze. On the other hand, FAD-AOXs offer irreversible oxidation of  
48 alcohols with the aid of molecular O<sub>2</sub> and a flavin cofactor tightly bound to the enzyme<sup>17,20</sup>.

49  
50 Copper radical oxidases (CROs) belonging to the Auxiliary Activity Family 5 subfamily 2  
51 (AA5\_2) – according to the CAZy classification<sup>21,22</sup> ([www.cazy.org](http://www.cazy.org)) – represent a promising  
52 alternative to these two systems. They are organic cofactor free enzymes bearing two redox  
53 centers: a copper ion and a 3'-(S-cysteinyl)-tyrosine (Cys-Tyr) free radical<sup>23</sup>. They catalyze the  
54 oxidation of alcohols to aldehyde with the concomitant reduction of O<sub>2</sub> to H<sub>2</sub>O<sub>2</sub> (Scheme 1). They  
55 are often use in conjugation with catalase – to remove deleterious H<sub>2</sub>O<sub>2</sub> – and peroxidase (*e.g.*  
56 horseradish peroxidase – HRP) for their activation<sup>24</sup>. For many years, the only characterized  
57 member from this family was the canonical galactose 6-oxidase (EC 1.1.3.9) from *Fusarium*  
58 *graminearum* (*FgrGalOx*)<sup>25</sup>. Recently, a new type of alcohol oxidases, was found in this family.  
59 These enzymes, from *Colletotrichum graminicola* (*CgrAlcOx*) & *C. gloeosporoides* (*CglAlcOx*),  
60 were described as competent aromatic- and aliphatic- primary alcohol oxidases<sup>26</sup>. Two  
61 homologues from *C. higginsianum* and *Magnaporthe oryzae* – anamorph *Pyricularia oryzae* –  
62 have also been described, but only tested on short-chain aliphatic-alcohols<sup>27</sup>. A paralogous enzyme  
63 from *C. graminicola* (*CgrAAO*) was recently reported to be highly active on aromatic alcohols  
64 (EC 1.1.3.7) and 5-hydroxymethylfurfural (HMF, EC 1.1.3.47), but lacked activity on long chain  
65 aliphatic alcohols<sup>28</sup>. Overall, the broad substrate scope covered by these recently characterized  
66 fungal enzymes highlights the catalytic potential within the AA5\_2 protein family. A striking  
67 example of such catalytic promiscuity was recently unveiled in a variant of the *FgrGalOx*,  
68 unlocking production of nitriles from alcohols in presence of ammonia<sup>29</sup>. Yet, despite their  
69 intrinsic and unique biocatalytic abilities, and in contrast to ADH and AOX systems<sup>19</sup> or the

70 archetypal *FgrGalOx* and its engineered variants that have been harnessed for multiple  
71 applications<sup>24,30–37</sup>, the CRO-AlcOx have hitherto received little attention as biocatalysts for the  
72 oxidation of industrially relevant alcohols.



73  
74 **Scheme 1: Reaction scheme of alcohol oxidation to aldehyde by CROs from the AA5\_2 subfamily.**  
75 The main states of the two redox centers (copper ion and Cys-Tyr free radical) are depicted in blue.  
76 Accessory enzymes commonly used to activate the CROs (*i.e.* peroxidase) and to remove deleterious H<sub>2</sub>O<sub>2</sub>  
77 (*i.e.* catalase) are shown in orange and green boxes respectively.

78  
79 Here, we present a new biocatalytic route for the production of odorant aldehydes, with a focus  
80 on industrially-relevant aromatic and long chain aliphatic compounds. We report for the first-time  
81 large-scale production of the *CgrAlcOx* and propose general guidelines for its use as green catalyst  
82 for the oxidation of primary long chain aliphatic alcohols. Combining biochemical assays and *in*  
83 *silico* modelling we provide unprecedented insights into the reaction determinants driving the  
84 formation of aldehyde and controlling the subsequent, potential and multifactorial overoxidation  
85 into carboxylic acid.

86

## 87 RESULTS

88

### 89 **Large-scale production of *CgrAlcOx* and analytical set up for bioconversion.**

90 Biotechnological application of enzyme is frequently hampered by low recombinant production  
91 yield. As a first step towards a scalable process, we developed larger-scale heterologous production  
92 of *CgrAlcOx* in bioreactor using the yeast *Pichia pastoris*, which yielded up to 250 mg of purified  
93 enzyme per liter of culture (Figure S1). The specific activities of both *CgrAlcOx* recombinant  
94 enzymes produced in flask and in bioreactor were similar (Figure S1D). The recombinant  
95 *CgrAlcOx* produced in bioreactor was further used in all the subsequent experiments described in  
96 the manuscript.

97 The analysis of reaction mixtures involving poorly water-soluble long chain aliphatic  
98 alcohols/aldehydes calls for the use of alternative methods than the indirect ABTS/HRP coupled  
99 assay, routinely used for CROs. To this end, we implemented a gas chromatography (GC)-FID  
100 analytical method. The first assays, run with the reference substrate benzyl alcohol (BnOH),  
101 confirmed the requirement of the accessory enzymes catalase and/or HRP, to fulfill complete  
102 conversion of BnOH<sup>38</sup> (Figure S2). Nevertheless and interestingly, we here showed that as little  
103 as 5 nM of catalase (Figure S2C) are enough to reach full conversion while the HRP must be added  
104 in quasi-stoichiometric amounts (relative to the AlcOx, *i.e.* in the  $\mu\text{M}$  range; Figure S2D).

105

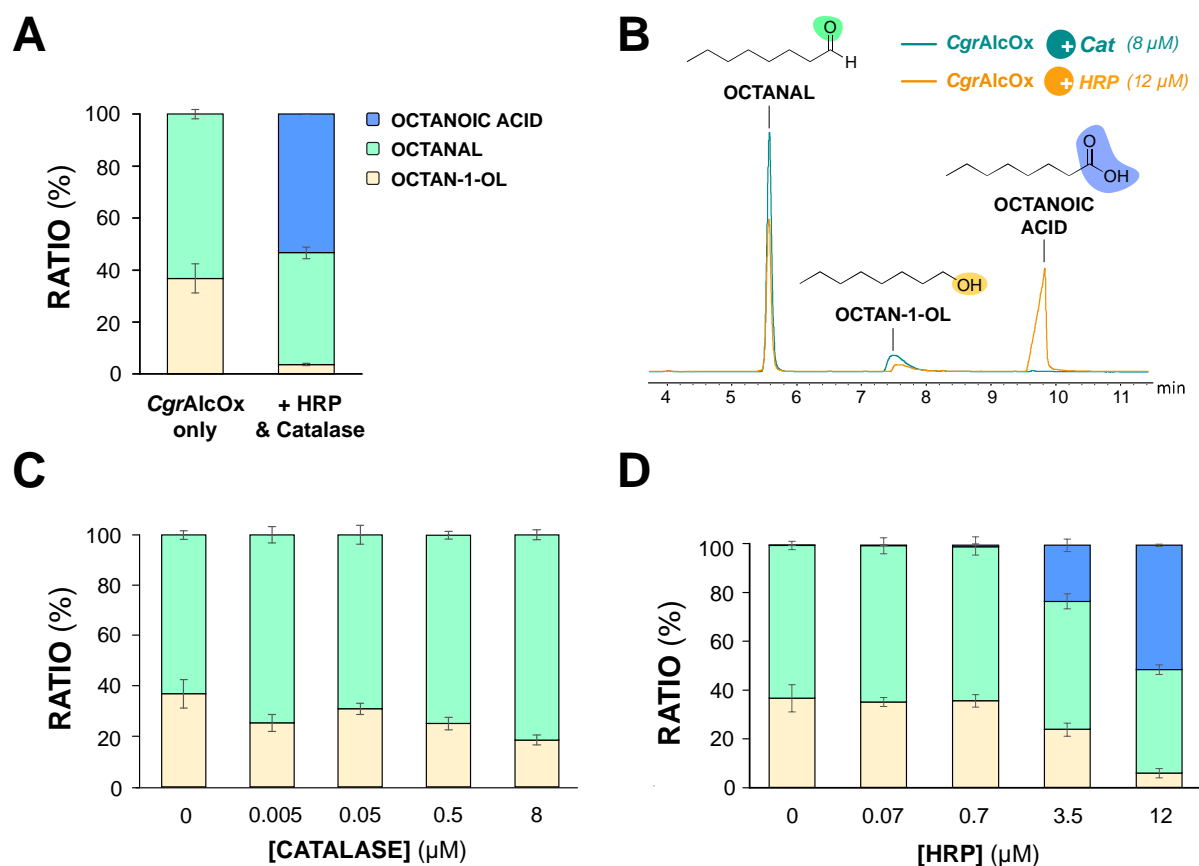
### 106 ***CgrAlcOx* is a competent catalyst for the full conversion of octan-1-ol.**

107 The next step was dedicated to the study of oxidation of octan-1-ol, often used as a model of  
108 non-activated primary long chain aliphatic alcohols<sup>9</sup>. The corresponding aldehyde, *i.e.* octanal, is  
109 a molecule with valuable aroma properties, naturally found in citrus essential oils<sup>14,39</sup>. As observed  
110 for the conversion of BnOH (Figure S2), the conversion of octan-1-ol to octanal did not surpass

111 60% with *CgrAlcOx* only, while almost full consumption of the substrate was reached with the  
112 addition of both accessory enzymes (12  $\mu\text{M}$  HRP and 0.5  $\mu\text{M}$  catalase) to the reaction (Figure 1A).  
113 Catalase, when added alone, showed only minor enhancement of *CgrAlcOx*-mediated conversion  
114 of octan-1-ol (Figure 1C), while HRP at high concentration ( $>3.5 \mu\text{M}$ ) exhibited a much more  
115 significant effect (Figure 1D). This result is the first report of complete turnover of an aliphatic  
116 unactivated primary alcohol by a CRO-AlcOx (with a turnover number – TON – of 3000). Indeed,  
117 previous attempts to convert the shorter alcohol butan-1-ol with the same enzyme (*CgrAlcOx*),  
118 but under non-optimized reaction conditions, failed to surpass 30 % conversion (TON = 1413)<sup>26</sup>.

119 Importantly, the formation of a new product, namely octanoic acid, was monitored and identified  
120 when HRP was added at high loading ( $> 3.5 \mu\text{M}$ ) (Figure 1A, B & D & S3). The presence of acid  
121 might indicate an overoxidation process, never highlighted before for any CRO-AlcOx. Of note,  
122 this product was not observed for any of the tested catalase concentrations (Figure 1C). Such  
123 overoxidation is undesired in the scope of flavors and fragrances inasmuch as the acid generates  
124 off-flavors and additional purification steps for isolation of the aldehyde. Understanding and  
125 control of this phenomenon is therefore required.





126

127 **Figure 1. *CgrAlcOx*-mediated oxidation of octan-1-ol.** (A) Oxidation of octan-1-ol by the  
 128 *CgrAlcOx* in the presence or absence of HRP (12 μM) and catalase (8 μM). (B) GC-FID  
 129 chromatograms of reactions catalyzed by *CgrAlcOx* in the presence or absence of HRP (12 μM)  
 130 or catalase (8 μM). (C & D) Oxidation of octan-1-ol by the *CgrAlcOx* with increasing  
 131 concentrations of catalase and HRP respectively. All reactions were incubated for 16 hours.  
 132 *CgrAlcOx* was used at 1 μM with 3 mM octan-1-ol. Error bars show s.d. (independent  
 133 experiments, n = 3).

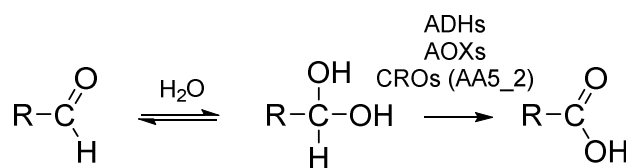
134

### 135 Investigation of the overoxidation process

136 To investigate the mechanism underlying the overoxidation observed in our enzymatic reactions,  
 137 two hypotheses were probed:

138 (1) The aldehyde is overoxidized to the acid by *CgrAlcOx* via a *geminal*-diol (*gem*-diol)  
139 intermediate that would act as a secondary substrate (Scheme 2). This oxidation pathway is a  
140 plausible route<sup>40,41</sup>, as notably reported for some ADHs<sup>42,43</sup>, FAD-AOXs<sup>17,44</sup>, AA5\_2 GalOx<sup>45-49</sup>  
141 and AA5\_1<sup>50</sup> (glyoxal oxidases, GLOX, EC 1.2.3.15).

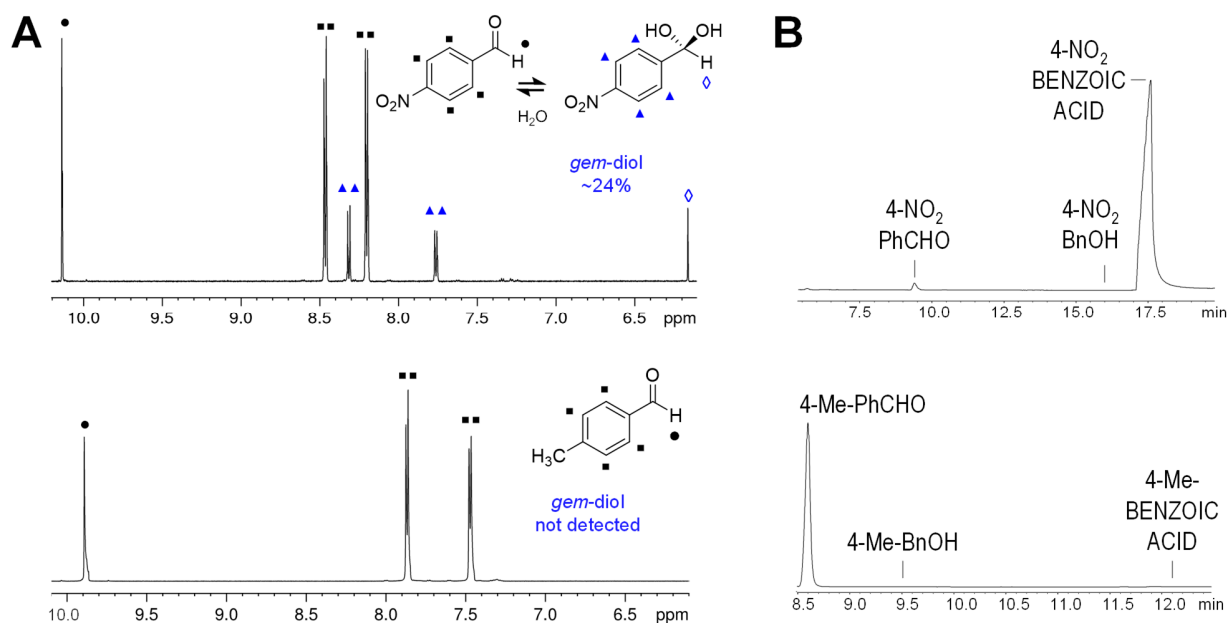
142 (2) The aldehyde is overoxidized *via* a non-enzymatic mechanism or by the accessory enzymes  
143 (*i.e.* HRP and/or catalase) added into the reaction.



144  
145 **Scheme 2. Aldehyde oxidation to carboxylic acid via non-enzymatic hydration followed by**  
146 **enzymatic oxidation of the *gem*-diol intermediate.**

147 In the *gem*-diol hypothesis, as suggested in a previous study<sup>38</sup>, the mechanism would be substrate  
148 dependent. Indeed, some aldehydes (such as aliphatic aldehydes) are more prone than others to  
149 undergo hydration<sup>51</sup>. For instance, hydration constant ( $K_H$ ) values of 0.75 M<sup>-1</sup> vs 0.01 M<sup>-1</sup> were  
150 reported<sup>38</sup> for hexanal and PhCHO, respectively<sup>52,53</sup>. Of note,  $K_H$  values for octanal and hexanal  
151 are expected to be similar as the increase in carbon chain-length has a minor effect<sup>52,54</sup>. To probe  
152 this first hypothesis, starting with the benchmark substrate BnOH, and on the basis of former  
153 studies<sup>44,48,55</sup>, we firstly chose two BnOH analogues bearing either an electron-withdrawing group  
154 (EWG) or an electron-donating group (EDG) to affect the  $K_H$  value. <sup>1</sup>H-NMR analysis confirmed  
155 that the *gem*-diol was formed (24 %) in aqueous conditions only for the aldehyde bearing an EWG  
156 (4-nitro-benzaldehyde; 4-NO<sub>2</sub>-PhCHO) in contrast to 4-methyl-benzaldehyde (4-Me-PhCHO)  
157 (Figure 2A). Subsequently, we carried out conversion experiments using these BnOH analogues  
158 as substrates, in the presence of *CgrAlcOx*, HRP and catalase. Quasi-full conversion to the  
159 corresponding carboxylic acid was obtained for 4-NO<sub>2</sub>-BnOH while in the same conditions 4-Me-

160 BnOH conversion produced only aldehyde (Figure 2B & S3C-D), steering towards the *gem*-diol  
161 hypothesis (see discussion for more details).



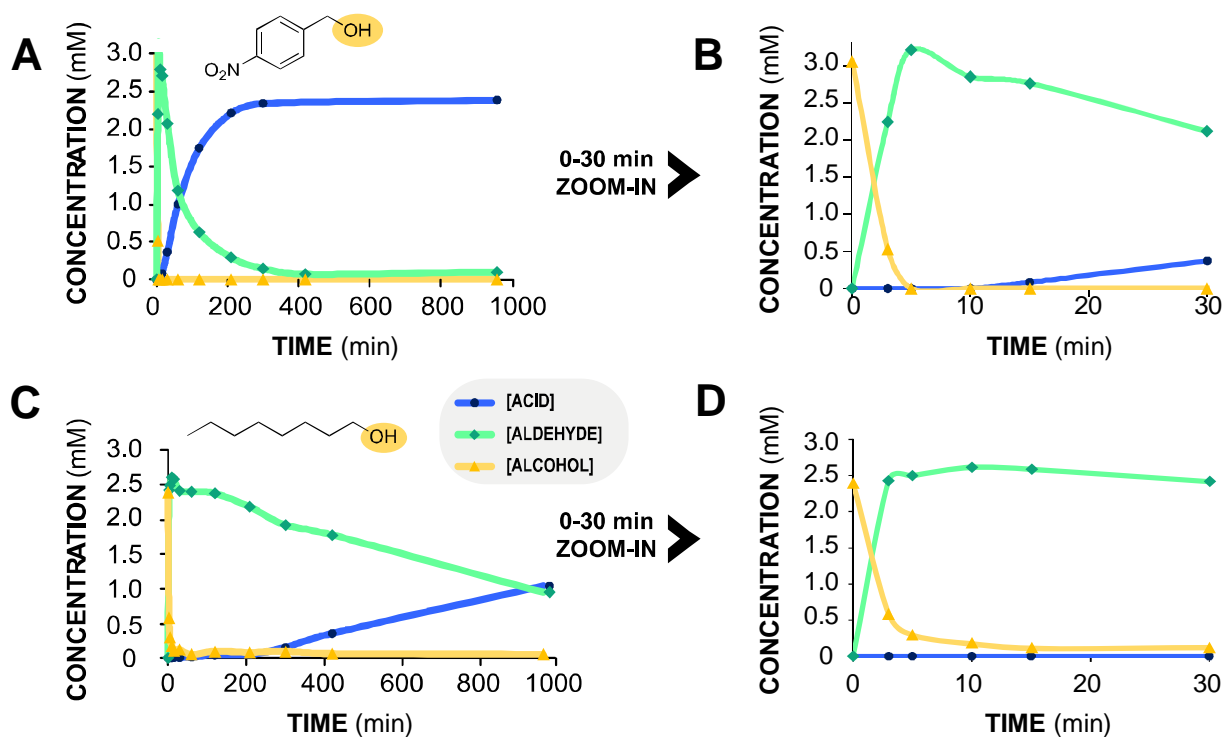
162  
163

164 **Figure 2. Conversion of 4-NO<sub>2</sub>-BnOH and 4-Me-BnOH by the *CgrAlcOx*.** (A) <sup>1</sup>H-NMR  
165 spectra of the aldehydes 4-NO<sub>2</sub>-PhCHO and 4-Me-PhCHO in aqueous media. (B) GC-FID  
166 chromatograms of 4-NO<sub>2</sub>-BnOH and 4-Me-BnOH (3 mM each) conversions by the *CgrAlcOx* (1  
167 μM) incubated for 16 hours in the presence of HRP (12 μM) and catalase (0.5 μM). In panel B,  
168 the retention time of the substrates and oxidation products is displayed in plain text.

169 Time course monitoring of 4-NO<sub>2</sub>-BnOH oxidation by the *CgrAlcOx* (supported by both  
170 accessory enzymes) revealed that the alcohol was readily converted to aldehyde within five  
171 minutes (Figure 3A & B), while the overoxidation product was only detected after 30 minutes of  
172 reaction. Incubation of the aldehyde 4-NO<sub>2</sub>-PhCHO for 16 hours with only HRP (12 μM) or  
173 catalase (8 μM) showed no oxidation to the carboxylic acid form (Figure S4). Altogether, these  
174 experiments indicate a *CgrAlcOx*-mediated aldehyde oxidation. Nevertheless, support of the

175 *CgrAlcOx* by both accessory enzymes is required to observe full conversion to the acid, providing  
 176 also a more rapid reaction than with one or the other accessory enzyme added individually (Figure  
 177 S5). Noteworthy, the time course consumption of the aldehyde 4-NO<sub>2</sub>-PhCHO appeared to be  
 178 very similar whether the latter was produced *in situ* (Figure 3A) or added as initial substrate (Figure  
 179 S5D).

180

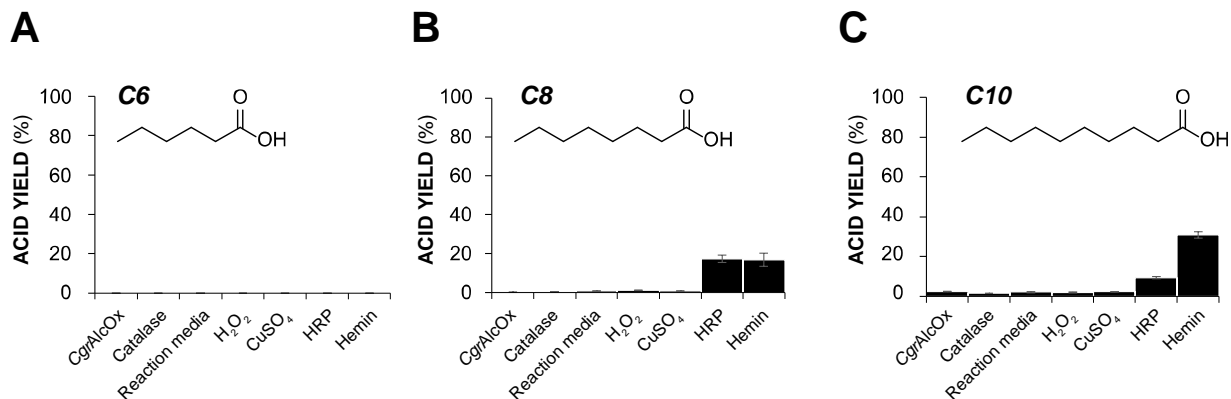


181  
 182 **Figure 3. Time course of 4-NO<sub>2</sub>-BnOH (A & B) and octan-1-ol (C & D) oxidation by the**  
 183 ***CgrAlcOx* (1 μM) supported by HRP (12 μM) and catalase (0.5 μM).** Panels B & D are zoom-  
 184 in views (0-30 minutes) of panels A & C, respectively. Reactions contained 3 mM substrates. The  
 185 legend in panel C applies for all panels. Each time course is the result of multiple replicates of the  
 186 same reaction stopped at different time points.

187 Based on the results gathered on the model benzyl-alcohol derivatives, we then probed the  
188 reactivity of some long chain aliphatic compounds. <sup>1</sup>H-NMR data confirmed the existence of  
189 hydrated *gem*-diol form for hexanal (C6; ~ 48 % of *gem*-diol) and octanal (C8; ~ 45 %) (Figure  
190 S6), however solubility of decanal (C10) in D<sub>2</sub>O was too poor to monitor a suitable signal. Time  
191 course analysis of octan-1-ol oxidation showed a very fast full conversion (*i.e.* 15 minutes) of  
192 octan-1-ol to octanal (Figure 3C & D) followed by a lag-phase of two to five hours before the  
193 detection of overoxidation to the acid. In contrast to 4-NO<sub>2</sub>-BnOH overoxidation, only partial  
194 conversion to the acid form was reached after 16 hours of reaction with both accessory enzymes.

195 To elucidate the origin of overoxidation for each substrates and ensure control over it in applied  
196 settings, we incubated in parallel reactions the different aldehydes during 16 hours, in various  
197 conditions: (a) in buffer, (b) with *CgrAlcOx*, (c) with the accessory enzymes (*i.e.* HRP or catalase)  
198 (d) with a set of oxidants likely to be present in the reaction mixture *i.e.* H<sub>2</sub>O<sub>2</sub> (released during  
199 *CgrAlcOx* turnover), free-copper (the first redox-catalytic center of the *CgrAlcOx*), and free-  
200 hemin (the redox-cofactor of the HRP). For long chain aliphatic aldehydes, the production of acid  
201 seems correlated with the carbon chain length: no oxidation was observed with C6 (Figure 4A &  
202 S7), whereas C8 and C10 aldehydes were partially oxidized to the corresponding carboxylic acid  
203 after 16 hours of incubation (Figure 4B, 4C, S7 & Table S1). Also, in contrast to the *CgrAlcOx*-  
204 dependent overoxidation of 4-NO<sub>2</sub>-PhCHO, the overoxidation of C8 and C10 aldehydes could be  
205 observed in the presence of HRP alone (Figure 4B, 4C & Figure S8). Keeping in mind that it is  
206 well-known that heme encased within HRP is itself an oxidant<sup>56</sup>, we performed control reactions.  
207 When HRP was replaced with free hemin we observed a similar oxidation of the C8 and C10  
208 aldehydes (Figure 4B & C) suggesting that the oxidation of long chain aliphatic aldehydes in

209 presence of HRP might be independent from its peroxidase activity but more likely due to the  
210 presence of its cofactor.

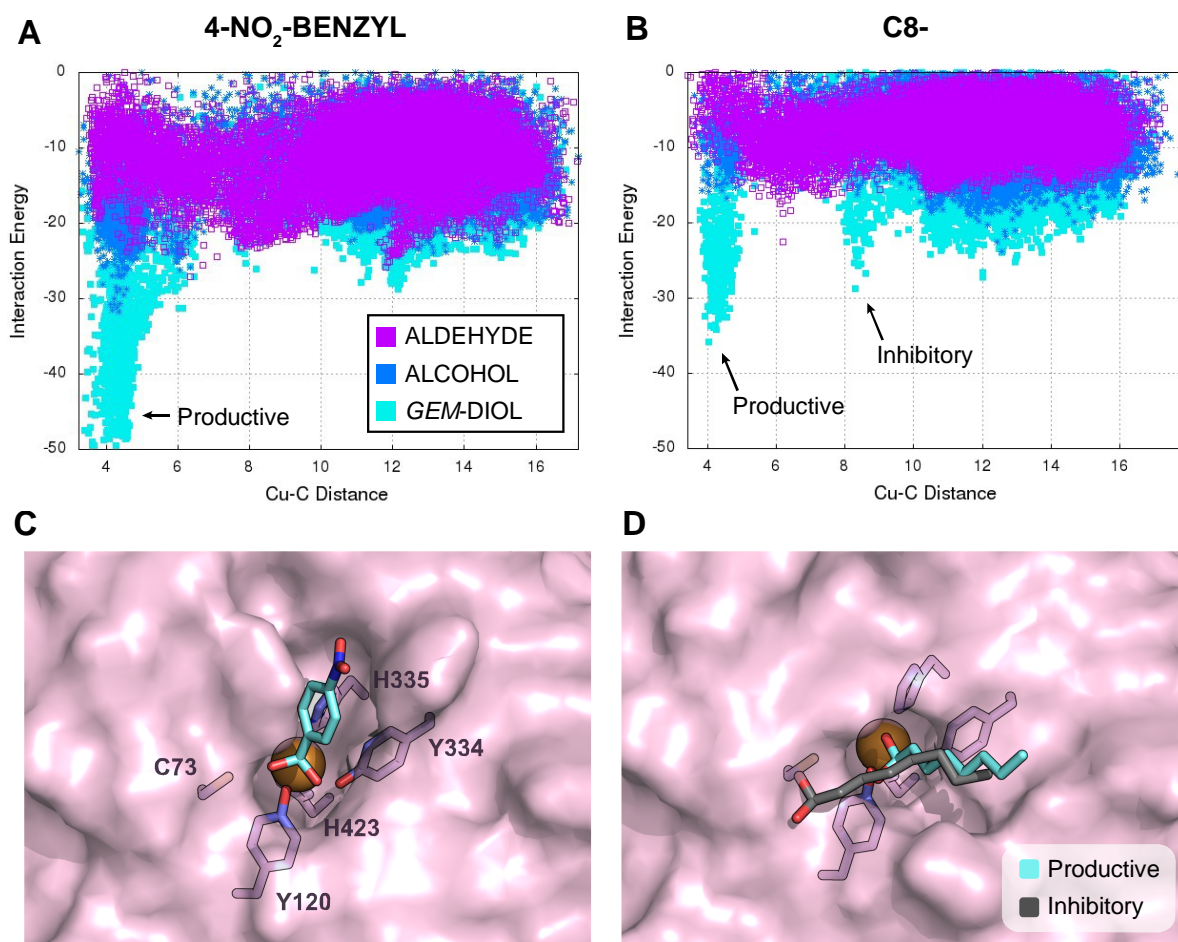


211  
212 **Figure 4. Yield of carboxylic acid detected after incubation of (A) hexanal, (B) octanal, and**  
213 **(C) decanal with various reagents.** All reactions were carried out in sodium phosphate buffer (50  
214 mM, pH 8) at 23°C, under stirring (190 rpm), and incubated for 16 hours. The reaction mixture  
215 contained 3 mM aldehyde and one of the following enzymatic or inorganic reagent: *CgrAlcOx* (1  
216 μM), catalase (8 μM), H<sub>2</sub>O<sub>2</sub> (3 mM), CuSO<sub>4</sub> (1 μM), HRP (12 μM) or hemin (10 μM). Reactions  
217 were monitored by GC-FID and results expressed in percentage of acid compared to initial quantity  
218 of aldehyde added. Error bars show s.d. (independent experiments, n = 3). Extended set of data is  
219 available in Table S1.

220 To get a deeper understanding of the distinctive role of aldehyde and *gem*-diol forms in CRO-  
221 AlcOx catalysis, we carried out molecular modeling analyses.

222 **Molecular modeling provides computational evidences for long chain aliphatic *gem*-diols**  
223 **inhibition and suggests substrate induced-fit into *CgrAlcOx* active site.**

224 Protein Energy Landscape Exploration (PELE)<sup>57,58</sup> was applied to simulate ligand-protein  
225 interaction and predict optimal docking of 4-NO<sub>2</sub>-benzyl- and octan- derivatives – *i.e.* alcohols,  
226 aldehydes and *gem*-diols – into *CgrAlcOx* active site (PDB 5C92<sup>26</sup>; Figure 5) As expected,  
227 aldehydes did not show favorable energy profiles, suggesting a poor binding of both benzyl- and  
228 long chain aliphatic aldehydes when they are non-hydrated (Figure 5A-B & S9). Alcohols showed  
229 plausible interaction energies at the proximity of copper ion (4 Å Cu-C distances), although more  
230 nuanced for octan-1-ol compared to BnOH and 4-NO<sub>2</sub>-BnOH. *Gem*-diols derivatives showed the  
231 lowest interaction energy, next to the copper region (Figure 5A & B), likely suggesting binding of  
232 these molecules (Figure 5C & D). In the case of octanal *gem*-diol an alternative binding position,  
233 located at ~ 8 Å from the copper ion (Figure 5B & D), suggests a possible “non-productive”  
234 binding. Overall, catalysis and computational studies suggest that *gem*-diols display favorable  
235 properties for binding into *CgrAlcOx* active site, yet with different outcomes. Indeed, in the case  
236 of benzyl derivatives *gem*-diols, *in vitro* experiments indicate that this binding leads to an  
237 overoxidation to carboxylic acid. In contrast, for unactivated aliphatic substrates, octanal-derived  
238 *gem*-diols most probably cause enzyme inhibition through a non-productive binding. This  
239 conclusion is supported by previous observations of impeded conversions of shorter aliphatic  
240 alcohols<sup>26</sup> and inhibition phenomenon by aliphatic aldehydes<sup>38</sup>. Accordingly, we observed an  
241 inhibitory effect of exogenously added octanal on *CgrAlcOx*-mediated oxidation of octan-1-ol  
242 (IC<sub>50</sub> = 3.19 mM ± 0.19; Figure S10).



243  
 244 **Figure 5. PELE's interaction energy plots for 4-NO<sub>2</sub>-benzyl-alcohol (A) and C8-alcohol (B),**  
 245 **aldehyde and gem-diol within *CgrAlcOx* active site and corresponding docking for the gem-**  
 246 **diols derivatives (C & D). Y axis PELE's interaction energy (in kcal.mol<sup>-1</sup>). X axis distance (in**  
 247 **Å) of the carbon (hosting the alcohol or carbonyl groups) to the Cu metal ion (shown as an orange**  
 248 **sphere in panels C and D). Copper coordination residues are shown by transparency in light purple**  
 249 **in panels C and D. The residues numbering shown in panel C applies for panel D likewise.**

250 PELE's simulations also revealed a possible substrate-induced fit mechanism in the active site  
 251 of the *CgrAlcOx*. Indeed, models suggest that the side chains of hydrophobic residues at the  
 252 entrance of the active site pocket such as W39, F138, M173 and F303 could undergo a slight  
 253 rotation (Figure S11A) to favor the binding of 4-NO<sub>2</sub>-BnOH. The active site topology is similar



254 whether the enzyme is substrate-free (Figure S11B) or in complex with octan-1-ol (Figure S11C)  
255 or BnOH (Figure S11D) while a wider pocket is visible in the case of 4-NO<sub>2</sub>-BnOH (Figure S11E).  
256 Such flexibility in the active site could play a significant role in the ability of *CgrAlcOx* to accept  
257 a broad range of substrates.

258 During the course of PELE modelling experiments, we also probed the recognition by *CgrAlcOx*  
259 of various aliphatic alcohols with chain lengths ranging from C2 to C10. A clear trend stood out:  
260 the longer the chain length the lower the binding energy (see below). These simulations prompted  
261 us to verify this trend by enzymatic assays.

262 The determination of kinetic parameters (Table 1 & Figure S12) revealed that while  $k_{cat}$  values  
263 for C7-C10 alcohols remained constant, the  $K_m$  values showed a slight but constant decrease with  
264 the increase in aliphatic chain length, a trend previously observed for shorter alcohols (C2-C7)<sup>26</sup>.  
265 As a comparative control, we verified that the kinetic parameters for C7 alcohol determined here  
266 and by Yin and colleagues<sup>26</sup> were similar.

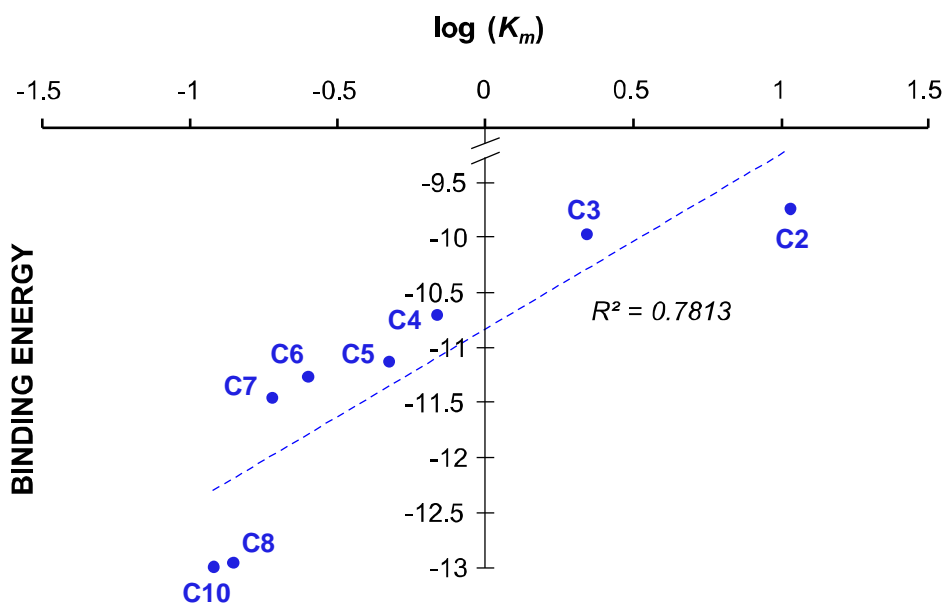
267  
268 **Table 1. Kinetic parameters of *CgrAlcOx* for several long chain aliphatic alcohols**  
269 **determined by the spectrophotometric ABTS/HRP coupled assay using 1 nM *CgrAlcOx*.**

Substrate	$k_{cat}$ (s <sup>-1</sup> )	$K_m$ (mM)	$k_{cat}/K_m$ (s <sup>-1</sup> .M <sup>-1</sup> )	Reference
Heptan-1-ol	100 ± 1	0.19 ± 0.01	5.3 x 10 <sup>5</sup>	Yin <i>et al.</i> <sup>26</sup>
	85.8 ± 1.016	0.19 ± 0.01	4.52 x 10 <sup>5</sup>	This work
Octan-1-ol	84.4 ± 1.3	0.14 ± 0.01	6.03 x 10 <sup>5</sup>	This work
Decan-1-ol	87.5 ± 2.2	0.12 ± 0.02	7.29 x 10 <sup>5</sup>	This work

270  
271 Attempting to relate experimental kinetic parameters to docking results, a few facts need to be  
272 laid out. The characteristic ‘ping-pong’ CRO’s catalytic cycle can be divided into two half-

273 reactions, a reductive half-reaction that entails enzyme active site reduction upon substrate  
274 oxidation, and a subsequent oxidative half-reaction where the enzyme is re-oxidized into its initial  
275 state while O<sub>2</sub> is reduced into H<sub>2</sub>O<sub>2</sub>. Studies performed on the *FgrGalOx* indicate that the oxidative  
276 half-reaction is not rate-limiting for AA5\_2s<sup>59,60</sup>, implying that  $k_{cat}$  reflects directly the rate of the  
277 reductive half-reaction. Furthermore, the facts that the  $k_{cat}$  value is not impacted by the nature of  
278 the oxidized substrate (Table 1), and is theoretically independent from the  $K_d$ , indicate that once  
279 the substrate is bound, the chemical reaction (*i.e.* CH<sub>2</sub>-OH → CHO) occurs at the same rate-  
280 limiting speed. All these considerations allow us to predict that variations in  $K_m$  and  $K_d$  values  
281 should be directly correlated, meaning that the observed decrease in  $K_m$  for longer chain lengths  
282 should reflect an increase in affinity. The correlation observed when plotting PELE's substrate  
283 binding energy for C2 to C8, and C10 straight chain saturated primary alcohols against  
284 experimental log ( $K_m$ ) values obtained here and previously<sup>26</sup> provides support to our simulation  
285 results and further suggests that the observed decrease in  $K_m$  for longer chain lengths may reflect  
286 an increase in affinity ( $K_d$ ) (Figure 6).

287



288  
 289 **Figure 6. Relationship between the average (top quartile) binding energies (C-Cu distances**  
 290 **< 4Å) determined by PELE and experimental log ( $K_m$ ) values for C2 to C8, and C10 straight**  
 291 **chain saturated primary alcohols with *CgrAlcOx*.**

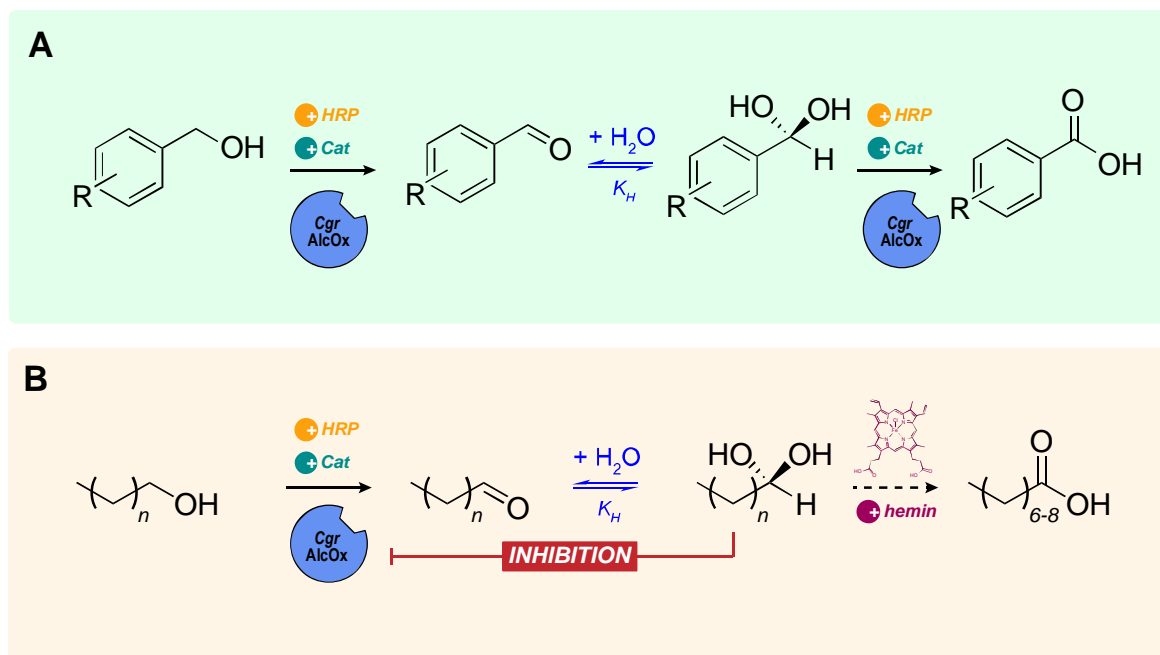
292  
 293 **Preparative-scale experiment**

294  
 295 To support the industrial applicability of *CgrAlcOx* catalyst, the knowledge acquired in the  
 296 present study was harnessed in a scaled-up experiment. To this end, we harvested the supernatant  
 297 of a *CgrAlcOx*-producing *P. pastoris* bioreactor and used it directly as crude enzyme solution.  
 298 One liter of crude enzyme was mixed to 2 g of octan-1-ol and allowed to react during 30 min to  
 299 limit overoxidation. After extraction with organic solvent, GC analysis revealed that 0.72 g of  
 300 octanal, 0.61 g of octan-1-ol and 0.03 g of octanoic acid were recovered. Interestingly, a parallel  
 301 reaction run with the same concentrations of substrate and accessory enzymes but at 10 mL volume  
 302 resulted in almost full conversion into aldehyde (92 % of C8ALD; 4.1 % of C8OH and 3.6 % of  
 303 C8AC), suggesting that the limited rate of conversion observed for the gram-scale experiment  
 304 might be due to experimental constraints (*e.g.* stirring, vessel etc.) and should be further optimized.

305 **DISCUSSION**  
306

307 In the current context, biotechnologies constitute the most promising alternative for the  
308 production of long chain aliphatic aldehydes as odorants in a flavors and fragrances market  
309 affected by an increasing demand for green and/or natural products that traditional production  
310 means cannot provide<sup>61,62</sup>. We herein demonstrate that a fungal CRO-AlcOx can achieve full  
311 conversion of some long chain aliphatic alcohols (*i.e.* hexan-1-ol and octan-1-ol) to yield the  
312 corresponding industrially-relevant aldehydes, within a few minutes, under mild conditions: water  
313 as solvent and O<sub>2</sub> as co-substrate. To the best of our knowledge, very few studies have reported  
314 the efficient conversion of unactivated long chain aliphatic alcohols. A recent contribution to this  
315 field indicates that a mutant from a FAD-dependent choline oxidase from *Arthrobacter*  
316 *cholorphenolicus* exhibited activity on some long chain aliphatic alcohols, with best performance  
317 on C4-C7 substrates<sup>18</sup>. The authors reported for this mutant a  $k_{cat}/K_m$  value on hexan-1-ol 1000-  
318 fold lower than for the *CgrAlcOx* and described full conversion of C6-C9 long chain aliphatic  
319 alcohols (10 mM) within 24 hours at 30°C, using 1 mg.mL<sup>-1</sup> of enzyme, with an approximative  
320 turnover frequency of  $7 \times 10^{-3} \text{ s}^{-1}$ . Comparatively, the *CgrAlcOx* was here used at 52 µg.mL<sup>-1</sup> to  
321 convert C6 and C8 alcohols (3 mM) in 15 minutes at 23°C exhibiting a turnover frequency of 3.3  
322 s<sup>-1</sup>. These promising results prompted us to attempt a gram scale reaction, which lead to the  
323 recovery of 0.72 g of octanal using a crude *CgrAlcOx* from bioreactor supernatant. This first proof  
324 of concept highlights the potential of CRO-AlcOx as biocatalysts for the production of long chain  
325 aliphatic aldehydes.

326 In this study, we also provide insights into the mechanism of the *CgrAlcOx* by comparing the  
327 oxidation of benzyl alcohol and derivatives and long chain aliphatic alcohols (Figure 7).



329

330 **Figure 7. Overview of the proposed oxidation mechanism by CgrAlcOx of benzyl alcohol (A)**  
 331 **and derivatives and long chain aliphatic alcohols (B).**

332 It is now well established that recombinant CROs require accessory enzymes to harness their  
 333 full potential: catalase for protection against H<sub>2</sub>O<sub>2</sub> and HRP for activation, the main resting-state  
 334 of the enzyme being inactivated<sup>63-65</sup>. Yet, as reported for GalOx, a minor fraction of the enzyme  
 335 pool is activated and likely explain the basal level of conversion observed without HRP or catalase,  
 336 before reaching an inactivated form due to the H<sub>2</sub>O<sub>2</sub> effect or undergoing “off-cycle  
 337 inactivation”<sup>66</sup>. Here, results suggest different requirement in accessory enzymes according to the  
 338 substrate to be oxidized. Indeed, rapid conversions require both HRP and catalase, confirming that  
 339 the two accessory enzymes are not interchangeable but bring distinct improvement to the  
 340 reaction<sup>38</sup>. Long-chain unactivated aliphatic substrates can only be fully converted by providing  
 341 high amount of HRP coupled to catalytic amount of catalase. This observation is likely related to  
 342 the inhibition by long chain aliphatic *gem*-diols resulting from the hydration of aldehydes products

343 (see discussion below). Although the molecular mechanism of activation of CROs needs to be  
344 better understood, it is clear that HRP acts as an oxidizing agent to restore the active form of the  
345 enzyme bearing the  $\text{Cu}^{2+}$  ion and the crosslinked Cys-Tyr free radical<sup>24,49</sup>. The stoichiometric  
346 proportion of HRP needed suggests a protein-protein interaction rather than a catalytic reaction<sup>67</sup>.  
347 It is worth noting that peroxidases are also routinely used to activate AA5\_1 GLOXs<sup>68,69</sup> pointing  
348 out a common activation mechanism of CROs.

349 The present work sheds light on the overoxidation reaction occurring during AlcOx catalysis.  
350 This reaction seems directly linked to the propensity of the produced aldehydes to form *gem*-diols  
351 upon hydration, which can be used as substrates in a late subsequent reaction, yielding the  
352 corresponding carboxylic acids. *Gem*-diols exist in equilibrium with their aldehyde counterparts  
353 but are often unfavored unless the carbonyl function is destabilized. For instance, electron-  
354 attracting substituents, such as  $\text{NO}_2$ , are known to disturb the dipole at the carbonyl group and  
355 thence, foster the nucleophilic addition of  $\text{H}_2\text{O}$ <sup>53</sup>. We show here that benzylic-aldehydes, when  
356 prone to form *gem*-diols (*i.e.* 4- $\text{NO}_2$ -PhCHO), are oxidized into carboxylic acid by the AlcOx  
357 whereas, when stabilized in their carbonyl form (*i.e.* 4-MePhCHO), are not further processed by  
358 the enzyme. However, the latter condition is not necessarily sufficient *per se*, since the presence  
359 of the substituting group may also affect the intrinsic reactivity of the carbon undergoing catalysis.  
360 Long chain aliphatic aldehydes are also susceptible to form *gem*-diols. However, our results  
361 suggest that these *gem*-diols are not oxidized by the AlcOx, and likely yield inhibitory binding at  
362 the active site of the enzyme. Yet, partial oxidation to the carboxylic acid, promoted by  
363 HRP/hemin, has been observed for  $>\text{C}_6$  aldehydes and seems therefore independent from  
364 *Cgr*AlcOx. This might account for a phenomenon related to the so-called “autoxidation”, a radical  
365 chain process mediated by oxygen, and favored by a large number of catalysts, hemin (free or

366 bound to HRP) being likely one of them<sup>70,71</sup>. A catalytic action of HRP is unlikely in the  
367 conversions we performed with *CgrAlcOx* and octan-1-ol, as H<sub>2</sub>O<sub>2</sub> should be dismutated *in-situ*  
368 by the catalase. It is however difficult to evaluate the amount of H<sub>2</sub>O<sub>2</sub> that would potentially  
369 accumulate in the reaction due to multiple crossed-production and consumption fluxes.

370 Other AA5\_2 CROs have shown evidence of *gem*-diol-dependent overoxidation such as the  
371 GalOx<sup>47,48</sup> or the raffinose-specific galactose oxidases from *C. graminicola*<sup>72</sup> and *Penicillium*  
372 *rubens*<sup>73</sup>. Nevertheless, not all the CROs appear to exhibit this overoxidation phenomenon, such  
373 as the *CgrAAO* that selectively oxidizes the primary alcohol function of HMF yielding as single  
374 end product the bis-aldehyde compound 2,5-diformylfuran despite the presence of *gem*-diol<sup>28</sup>. The  
375 formation of carboxylic acid can be either an unwanted product in the case of flavors and  
376 fragrances, or a sought after compound for applications in synthetic organic chemistry<sup>74</sup>. Fine  
377 tuning of reaction conditions (*i.e.* reaction length, substrate choice, quantity of accessory enzymes  
378 added, pH) allows steering the reaction towards either aldehyde or carboxylic acid. In this regard,  
379 the *CgrAlcOx* could be an efficient “all-in one” catalyst for direct oxidation of some benzylic-  
380 alcohols or other aromatic alcohols prone to form *gem*-diols to carboxylic acids. In contrast,  
381 formation of long chain aliphatic *gem*-diols should be avoided to prevent inhibition.

382 Building on a previously exposed hypothesis<sup>38</sup>, we showed here that the conversion yield of  
383 unactivated aliphatic alcohol is limited by an inhibition phenomenon that most likely involves the  
384 corresponding aliphatic *gem*-diols present in the reaction. Computational studies further strengthen  
385 this assumption, showing a possible inhibitory binding mode at the active site of the enzyme with  
386 octanal *gem*-diol. Such hypothesis is consistent with the fact that (i) larger amounts of accessory  
387 enzymes are required to convert efficiently octan-1-ol, since these enzymes activate the *CgrAlcOx*  
388 and probably allow to decrease the amount of inhibitory aldehyde or *gem*-diol (*via* conversion into

389 acid) and that (ii) *CgrAlcOx* is unable to oxidize aliphatic *gem*-diols into acids. The inhibition  
390 phenomenon seems common to all unactivated aliphatic alcohol as also reported previously for  
391 butan-1-ol and glycerol<sup>26</sup>.

392 Docking studies also highlighted a possible substrate-induced fit for 4-NO<sub>2</sub>-BnOH into  
393 *CgrAlcOx* active site as shown by a local twist of the side chain of key residues which could  
394 explain the strong substrate tolerance observed for this enzyme. In addition, despite 60 years of  
395 intensive research on this class of enzymes, almost exclusively focused on the *FgrGalOx*, such  
396 flexibility at the active site of AA5\_2s has not been reported and could contribute to the  
397 unexplained inability to obtain crystal structures of CRO-substrate complexes<sup>28</sup>.

398 Notwithstanding their intrinsic potential, CRO-AlcOx have been underexploited for alcohol  
399 oxidation, while efforts were focused on the carbohydrate-active *FgrGalOx* and mutants thereof<sup>19</sup>.  
400 Our study strives to unveil the potential of these promising catalysts and to outline the framework  
401 and boundaries of its scope of application. We herein provide guidelines for controlled oxidation  
402 of some long chain aliphatic and aromatic alcohols in the context of the flavors and fragrances  
403 market. The present work paves the way for scale-up experiments encouraged by high-yield  
404 protein production in bioreactor and mild-condition catalysis achieved with the *CgrAlcOx*  
405 biocatalyst. Engineering studies – sustained by a better understanding of the substrate-dependent  
406 oxidation initiated here – and process development such as immobilization and biphasic systems  
407 could foster the use of CRO-AlcOx for industrial-scale catalysis.



408 **SUPPORTING INFORMATION**

409 Material and methods, supplementary figures S1-S13, tables S1-S2, and supplementary  
410 references are provided in the Supporting Information associated file.

411

412 **AUTHOR CONTRIBUTIONS**

413

414 DR carried out most of the experimental work. BB provided guidance in the experimental work.  
415 DR and BB interpreted the data and wrote the manuscript; VG performed the *in silico* experiments,  
416 interpreted the corresponding results and was involved in the manuscript writing; MY drove the  
417 NMR experiments and the corresponding result interpretations, and was involved in the manuscript  
418 writing; MH and SG were involved in enzymes productions; VA was involved in the design of the  
419 gas chromatography experiments; HB and FL were involved in the study design and manuscript  
420 writing. JGB and ML conceptualized the study, supervised the work, and finalized the manuscript.  
421 All authors approved the final version of the manuscript.

422

423 **ACKNOWLEDGMENT**

424 This study was supported by the French National Agency for Research (“Agence Nationale de  
425 la Recherche”) through the “Projet de Recherche Collaboratif International” ANR-NSERC  
426 (FUNTASTIC project, ANR-17-CE07-0047), by the Natural Sciences and Engineering Research  
427 Council of Canada through the "Strategic Projects - Natural Resources and Energy - Project  
428 (STPGP) entitled "FUNTASTIC - Fungal copper-radical oxidases as new biocatalysts for the  
429 valorization of biomass carbohydrates and alcohols" and by the PID2019-106370RB-I00 grant  
430 from the Spanish Ministry of Innovation and Sciences. We are grateful to MANE & Fils and the  
431 “Association Nationale Recherche Technologie” (ANRT) for funding the PhD fellowship of D.R.

432 entitled “Discovery and structure-function study of new fungal copper radicals oxidases used as  
433 biocatalysts for the valorisation of alcohols and plant biomass.” This *Convention Industrielle de*  
434 *Formation par la Recherche* (CIFRE) grant no. 2017/1169 runs from 1 April 2018 to 1 April 2021.

435

436 **COMPETING INTEREST**

437 The authors declare that they have no competing interests.

438

439 **REFERENCES**

440

- 441 (1) Arends, I. W. C. E.; Gamez, P.; Sheldon, R. A. Green Oxidation of Alcohols Using  
442 Biomimetic Cu Complexes and Cu Enzymes as Catalysts. In *Advances in Inorganic*  
443 *Chemistry*; van Eldik, R., Reedijk, J., Eds.; Academic Press, **2006**; Vol. 58, pp 235–279.  
444 [https://doi.org/10.1016/S0898-8838\(05\)58006-1](https://doi.org/10.1016/S0898-8838(05)58006-1).
- 445 (2) Sadri, F.; Ramazani, A.; Massoudi, A.; Khoobi, M.; Tarasi, R.; Shafiee, A.; Azizkhani, V.;  
446 Dolatyari, L.; Joo, S. W. Green Oxidation of Alcohols by Using Hydrogen Peroxide in  
447 Water in the Presence of Magnetic Fe<sub>3</sub>O<sub>4</sub> Nanoparticles as Recoverable Catalyst. *Green*  
448 *Chemistry Letters and Reviews* **2014**, *7* (3), 257–264.  
449 <https://doi.org/10.1080/17518253.2014.939721>.
- 450 (3) Augugliaro, V.; Palmisano, L. Green Oxidation of Alcohols to Carbonyl Compounds by  
451 Heterogeneous Photocatalysis. *ChemSusChem* **2010**, *3* (10), 1135–1138.  
452 <https://doi.org/10.1002/cssc.201000156>.
- 453 (4) Ainembabazi, D.; Reid, C.; Chen, A.; An, N.; Kostal, J.; Voutchkova-Kostal, A.  
454 Decarbonylative Olefination of Aldehydes to Alkenes. *J. Am. Chem. Soc.* **2020**, *142* (2),  
455 696–699. <https://doi.org/10.1021/jacs.9b12354>.
- 456 (5) Rowe, D. Overview of Flavor and Fragrance Materials. In *Practical Analysis of Flavor and*  
457 *Fragrance Materials*; John Wiley & Sons, Ltd, **2011**; pp 1–22.  
458 <https://doi.org/10.1002/9781444343137.ch1>.
- 459 (6) Surburg, H.; Panten, J. *Common Fragrance and Flavor Materials: Preparation, Properties*  
460 *and Uses*; John Wiley & Sons, **2016**.
- 461 (7) Sell, C. S. *The Chemistry of Fragrances: From Perfumer to Consumer*; Royal Society of  
462 Chemistry, **2015**.
- 463 (8) Sheldon, R. A.; Brady, D. Broadening the Scope of Biocatalysis in Sustainable Organic  
464 Synthesis. *ChemSusChem* **2019**, *12* (13), 2859–2881.  
465 <https://doi.org/10.1002/cssc.201900351>.
- 466 (9) Corberán, V. C.; González-Pérez, M. E.; Martínez-González, S.; Gómez-Avilés, A. Green  
467 Oxidation of Fatty Alcohols: Challenges and Opportunities. *Applied Catalysis A: General*  
468 **2014**, *474*, 211–223. <https://doi.org/10.1016/j.apcata.2013.09.040>.
- 469 (10) Mudge, S. Fatty Alcohols – a Review of Their Natural Synthesis and Environmental  
470 Distribution. *Executive Summary of the Soap and Detergent Association* **2005**.
- 471 (11) Tsuzuki, S. Higher Straight-Chain Aliphatic Aldehydes: Importance as Odor-Active  
472 Volatiles in Human Foods and Issues for Future Research. *J. Agric. Food Chem.* **2019**, *67*  
473 (17), 4720–4725. <https://doi.org/10.1021/acs.jafc.9b01131>.
- 474 (12) Goswami, P.; Chinnadayala, S. S. R.; Chakraborty, M.; Kumar, A. K.; Kakoti, A. An  
475 Overview on Alcohol Oxidases and Their Potential Applications. *Applied Microbiology and*  
476 *Biotechnology* **2013**, *97* (10), 4259–4275. <https://doi.org/10.1007/s00253-013-4842-9>.
- 477 (13) Kohlpaintner, C.; Schulte, M.; Falbe, J.; Lappe, P.; Weber, J.; Frey, G. D. Aldehydes,  
478 Aliphatic. In *Ullmann's Encyclopedia of Industrial Chemistry*; American Cancer Society,  
479 **2013**. [https://doi.org/10.1002/14356007.a01\\_321.pub3](https://doi.org/10.1002/14356007.a01_321.pub3).
- 480 (14) Porat, R.; Deterre, S.; Giampaoli, P.; Plotto, A. The Flavor of Citrus Fruit. In *Biotechnology*  
481 *in Flavor Production*; John Wiley & Sons, Ltd, **2016**; pp 1–31.  
482 <https://doi.org/10.1002/9781118354056.ch1>.

- 483 (15) Zviely, M. Aroma Chemicals. In *Kirk-Othmer Encyclopedia of Chemical Technology*;  
484 American Cancer Society, **2012**; pp 1–33.  
485 <https://doi.org/10.1002/0471238961.0118151326220905.a01.pub2>.
- 486 (16) Winkler, M. Carboxylic Acid Reductase Enzymes (CARs). *Current Opinion in Chemical*  
487 *Biology* **2018**, *43*, 23–29. <https://doi.org/10.1016/j.cbpa.2017.10.006>.
- 488 (17) Pickl, M.; Fuchs, M.; Glueck, S. M.; Faber, K. The Substrate Tolerance of Alcohol  
489 Oxidases. *Applied Microbiology and Biotechnology* **2015**, *99* (16), 6617–6642.  
490 <https://doi.org/10.1007/s00253-015-6699-6>.
- 491 (18) Heath, R. S.; Birmingham, W. R.; Thompson, M. P.; Taglieber, A.; Daviet, L.; Turner, N.  
492 J. An Engineered Alcohol Oxidase for the Oxidation of Primary Alcohols. *ChemBioChem*  
493 **2019**, *20* (2), 276–281. <https://doi.org/10.1002/cbic.201800556>.
- 494 (19) Liu, J.; Wu, S.; Li, Z. Recent Advances in Enzymatic Oxidation of Alcohols. *Current*  
495 *Opinion in Chemical Biology* **2018**, *43*, 77–86. <https://doi.org/10.1016/j.cbpa.2017.12.001>.
- 496 (20) Kroutil, W.; Mang, H.; Edegger, K.; Faber, K. Biocatalytic Oxidation of Primary and  
497 Secondary Alcohols. *Advanced Synthesis & Catalysis* **2004**, *346* (2–3), 125–142.  
498 <https://doi.org/10.1002/adsc.200303177>.
- 499 (21) Lombard, V.; Golaconda Ramulu, H.; Drula, E.; Coutinho, P. M.; Henrissat, B. The  
500 Carbohydrate-Active Enzymes Database (CAZy) in 2013. *Nucleic Acids Research* **2014**, *42*  
501 (D1), D490–D495. <https://doi.org/10.1093/nar/gkt1178>.
- 502 (22) Levasseur, A.; Drula, E.; Lombard, V.; Coutinho, P. M.; Henrissat, B. Expansion of the  
503 Enzymatic Repertoire of the CAZy Database to Integrate Auxiliary Redox Enzymes.  
504 *Biotechnol Biofuels* **2013**, *6*, 41. <https://doi.org/10.1186/1754-6834-6-41>.
- 505 (23) Ito, N.; Phillips, S. E.; Stevens, C.; Ogel, Z. B.; McPherson, M. J.; Keen, J. N.; Yadav, K.  
506 D.; Knowles, P. F. Novel Thioether Bond Revealed by a 1.7 Å Crystal Structure of  
507 Galactose Oxidase. *Nature* **1991**, *350* (6313), 87–90. <https://doi.org/10.1038/350087a0>.
- 508 (24) T. Pedersen, A.; Birmingham, W. R.; Rehn, G.; Charnock, S. J.; Turner, N. J.; Woodley, J.  
509 M. Process Requirements of Galactose Oxidase Catalyzed Oxidation of Alcohols. *Organic*  
510 *Process Research & Development* **2015**, *19* (11), 1580–1589.  
511 <https://doi.org/10.1021/acs.oprd.5b00278>.
- 512 (25) Cooper, J. A. D.; Smith, W.; Bacila, M.; Medina, H. Galactose Oxidase from *Polyporus*  
513 *circinatus*, Fr. *J. Biol. Chem.* **1959**, *234* (3), 445–448.
- 514 (26) Yin, D.; Urresti, S.; Lafond, M.; Johnston, E. M.; Derikvand, F.; Ciano, L.; Berrin, J.-G.;  
515 Henrissat, B.; Walton, P. H.; Davies, G. J.; Brumer, H. Structure–Function Characterization  
516 Reveals New Catalytic Diversity in the Galactose Oxidase and Glyoxal Oxidase Family.  
517 *Nature Communications* **2015**, *6* (1). <https://doi.org/10.1038/ncomms10197>.
- 518 (27) Oide, S.; Tanaka, Y.; Watanabe, A.; Inui, M. Carbohydrate-Binding Property of a Cell Wall  
519 Integrity and Stress Response Component (WSC) Domain of an Alcohol Oxidase from the  
520 Rice Blast Pathogen *Pyricularia oryzae*. *Enzyme and Microbial Technology* **2019**, *125*, 13–  
521 20. <https://doi.org/10.1016/j.enzmictec.2019.02.009>.
- 522 (28) Mathieu, Y.; Offen, W. A.; Forget, S. M.; Ciano, L.; Viborg, A. H.; Blagova, E.; Henrissat,  
523 B.; Walton, P. H.; Davies, G. J.; Brumer, H. Discovery of a Fungal Copper Radical Oxidase  
524 with High Catalytic Efficiency towards 5-Hydroxymethylfurfural and Benzyl Alcohols for  
525 Bioprocessing. *ACS Catal.* **2020**. <https://doi.org/10.1021/acscatal.9b04727>.
- 526 (29) Vilím, J.; Knaus, T.; Mutti, F. G. Catalytic Promiscuity of Galactose Oxidase: A Mild  
527 Synthesis of Nitriles from Alcohols, Air, and Ammonia. *Angewandte Chemie* **2018**, *130*  
528 (43), 14436–14440. <https://doi.org/10.1002/ange.201809411>.

- 529 (30) Escalettes, F.; Turner, N. J. Directed Evolution of Galactose Oxidase: Generation of  
530 Enantioselective Secondary Alcohol Oxidases. *ChemBioChem* **2008**, *9* (6), 857–860.  
531 <https://doi.org/10.1002/cbic.200700689>.
- 532 (31) Matthey, A. P.; Sangster, J. J.; Ramsden, J. I.; Baldwin, C.; Birmingham, W. R.; Heath, R.  
533 S.; Angelastro, A.; Turner, N. J.; Cosgrove, S. C.; Flitsch, S. L. Natural Heterogeneous  
534 Catalysis with Immobilised Oxidase Biocatalysts. *RSC Adv.* **2020**, *10* (33), 19501–19505.  
535 <https://doi.org/10.1039/D0RA03618H>.
- 536 (32) Herter, S.; McKenna, S. M.; Frazer, A. R.; Leimkühler, S.; Carnell, A. J.; Turner, N. J.  
537 Galactose Oxidase Variants for the Oxidation of Amino Alcohols in Enzyme Cascade  
538 Synthesis. *ChemCatChem* **2015**, *7* (15), 2313–2317.  
539 <https://doi.org/10.1002/cctc.201500218>.
- 540 (33) Weissenborn, M. J.; Notonier, S.; Lang, S.-L.; Otte, K. B.; Herter, S.; Turner, N. J.; Flitsch,  
541 S. L.; Hauer, B. Whole-Cell Microtiter Plate Screening Assay for Terminal Hydroxylation  
542 of Fatty Acids by P450s. *Chemical Communications* **2016**, *52* (36), 6158–6161.  
543 <https://doi.org/10.1039/C6CC01749E>.
- 544 (34) McKenna, S. M.; Leimkühler, S.; Herter, S.; Turner, N. J.; Carnell, A. J. Enzyme Cascade  
545 Reactions: Synthesis of Furandicarboxylic Acid (FDCA) and Carboxylic Acids Using  
546 Oxidases in Tandem. *Green Chem.* **2015**, *17* (6), 3271–3275.  
547 <https://doi.org/10.1039/C5GC00707K>.
- 548 (35) Fuchs, M.; Tauber, K.; Sattler, J.; Lechner, H.; Pfeffer, J.; Kroutil, W.; Faber, K. Amination  
549 of Benzylic and Cinnamic Alcohols via a Biocatalytic, Aerobic, Oxidation–Transamination  
550 Cascade. *RSC Adv.* **2012**, *2* (15), 6262–6265. <https://doi.org/10.1039/C2RA20800H>.
- 551 (36) Fuchs, M.; Schober, M.; Pfeffer, J.; Kroutil, W.; Birner-Gruenberger, R.; Faber, K.  
552 Homoallylic Alcohols via a Chemo-Enzymatic One-Pot Oxidation–Allylation Cascade.  
553 *Advanced Synthesis & Catalysis* **2011**, *353* (13), 2354–2358.  
554 <https://doi.org/10.1002/adsc.201100380>.
- 555 (37) Rannes, J. B.; Ioannou, A.; Willies, S. C.; Grogan, G.; Behrens, C.; Flitsch, S. L.; Turner,  
556 N. J. Glycoprotein Labeling Using Engineered Variants of Galactose Oxidase Obtained by  
557 Directed Evolution. *J. Am. Chem. Soc.* **2011**, *133* (22), 8436–8439.  
558 <https://doi.org/10.1021/ja2018477>.
- 559 (38) Forget, S.; Xia, R. (Fan); Hein, J. E.; Brumer, H. Determination of Biocatalytic Parameters  
560 of a Copper Radical Oxidase Using Real-Time Reaction Progress Monitoring. *Org. Biomol.*  
561 *Chem.* **2020**. <https://doi.org/10.1039/C9OB02757B>.
- 562 (39) Surburg, H.; Panten, J. *Common Fragrance and Flavor Materials: Preparation, Properties*  
563 *and Uses*; John Wiley & Sons, 2006.
- 564 (40) Monti, D.; Ottolina, G.; Carrea, G.; Riva, S. Redox Reactions Catalyzed by Isolated  
565 Enzymes. *Chem. Rev.* **2011**, *111* (7), 4111–4140. <https://doi.org/10.1021/cr100334x>.
- 566 (41) Hollmann, F.; Arends, I. W. C. E.; Buehler, K.; Schallmeyer, A.; Bühler, B. Enzyme-  
567 Mediated Oxidations for the Chemist. *Green Chem.* **2011**, *13* (2), 226–265.  
568 <https://doi.org/10.1039/C0GC00595A>.
- 569 (42) Dong, J.; Fernández-Fueyo, E.; Hollmann, F.; Paul, C. E.; Pesic, M.; Schmidt, S.; Wang,  
570 Y.; Younes, S.; Zhang, W. Biocatalytic Oxidation Reactions: A Chemist’s Perspective.  
571 *Angew Chem Int Ed Engl* **2018**, *57* (30), 9238–9261.  
572 <https://doi.org/10.1002/anie.201800343>.
- 573 (43) Sigman, D. S. *The Enzymes*; Academic Press, **1992**; Vol. XX Mechanisms of Catalysis.  
574

- 575 (44) Martin, C.; Trajkovic, M.; Fraaije, M. Production of Hydroxy Acids through Selective  
576 Double Oxidation of Diols by a Flavoprotein Alcohol Oxidase. *Angewandte Chemie*  
577 *International Edition* **2020**, *59* (12), 4869–4872. <https://doi.org/10.1002/anie.201914877>.
- 578 (45) Kelleher, F. M.; Bhavanandan, V. P. Re-Examination of the Products of the Action of  
579 Galactose Oxidase. Evidence for the Conversion of Raffinose to 6''-Carboxyaffinose. *J.*  
580 *Biol. Chem.* **1986**, *261* (24), 11045–11048.
- 581 (46) Matsumura, S.; Kuroda, A.; Higaki, N.; Hiruta, Y.; Yoshikawa, S. Formation of Uronic  
582 Acid by Galactose Oxidase. *Chem. Lett.* **1988**, *17* (10), 1747–1750.  
583 <https://doi.org/10.1246/cl.1988.1747>.
- 584 (47) Parikka, K.; Tenkanen, M. Oxidation of Methyl  $\alpha$ -d-Galactopyranoside by Galactose  
585 Oxidase: Products Formed and Optimization of Reaction Conditions for Production of  
586 Aldehyde. *Carbohydrate Research* **2009**, *344* (1), 14–20.  
587 <https://doi.org/10.1016/j.carres.2008.08.020>.
- 588 (48) Birmingham, W. R.; Turner, N. J. A Single Enzyme Oxidative “Cascade” via a Dual-  
589 Functional Galactose Oxidase. *ACS Catal.* **2018**, *8* (5), 4025–4032.  
590 <https://doi.org/10.1021/acscatal.8b00043>.
- 591 (49) Parikka, K.; Master, E.; Tenkanen, M. Oxidation with Galactose Oxidase: Multifunctional  
592 Enzymatic Catalysis. *Journal of Molecular Catalysis B: Enzymatic* **2015**, *120*, 47–59.  
593 <https://doi.org/10.1016/j.molcatb.2015.06.006>.
- 594 (50) Whittaker, M. M.; Kersten, P. J.; Nakamura, N.; Sanders-Loehr, J.; Schweizer, E. S.;  
595 Whittaker, J. W. Glyoxal Oxidase from *Phanerochaete chrysosporium* Is a New Radical-  
596 Copper Oxidase. *J. Biol. Chem.* **1996**, *271* (2), 681–687.  
597 <https://doi.org/10.1074/jbc.271.2.681>.
- 598 (51) Buschmann, H.-J.; Fuldner, H.-H.; Knoche, W. The Reversible Hydration of Carbonyl  
599 Compounds in Aqueous Solution. Part I, The Keto/Gem-Diol Equilibrium. *Berichte der*  
600 *Bunsengesellschaft für physikalische Chemie* **1980**, *84* (1), 41–44.  
601 <https://doi.org/10.1002/bbpc.19800840109>.
- 602 (52) Li, Y.; Peterlin, Z.; Ho, J.; Yarnitzky, T.; Liu, M. T.; Fichman, M.; Niv, M. Y.; Matsunami,  
603 H.; Firestein, S.; Ryan, K. Aldehyde Recognition and Discrimination by Mammalian  
604 Odorant Receptors via Functional Group-Specific Hydration Chemistry. *ACS Chem Biol*  
605 **2014**, *9* (11), 2563–2571. <https://doi.org/10.1021/cb400290u>.
- 606 (53) Hilal, S. H.; Bornander, L. L.; Carreira, L. A. Hydration Equilibrium Constants of  
607 Aldehydes, Ketones and Quinazolines. *QSAR & Combinatorial Science* **2005**, *24* (5), 631–  
608 638. <https://doi.org/10.1002/qsar.200430913>.
- 609 (54) Buschmann, H.-J.; Dutkiewicz, E.; Knoche, W. The Reversible Hydration of Carbonyl  
610 Compounds in Aqueous Solution Part II: The Kinetics of the Keto/Gem-Diol Transition.  
611 *Berichte der Bunsengesellschaft für physikalische Chemie* **1982**, *86* (2), 129–134.  
612 <https://doi.org/10.1002/bbpc.19820860208>.
- 613 (55) Ferreira, P.; Hernández-Ortega, A.; Herguedas, B.; Rencoret, J.; Gutiérrez, A.; Martínez,  
614 M. J.; Jiménez-Barbero, J.; Medina, M.; Martínez, Á. T. Kinetic and Chemical  
615 Characterization of Aldehyde Oxidation by Fungal Aryl-Alcohol Oxidase. *Biochem J* **2010**,  
616 *425* (3), 585–593. <https://doi.org/10.1042/BJ20091499>.
- 617 (56) Xue, T.; Jiang, S.; Qu, Y.; Su, Q.; Cheng, R.; Dubin, S.; Chiu, C.-Y.; Kaner, R.; Huang, Y.;  
618 Duan, X. Graphene-Supported Hemin as a Highly Active Biomimetic Oxidation Catalyst.  
619 *Angewandte Chemie International Edition* **2012**, *51* (16), 3822–3825.  
620 <https://doi.org/10.1002/anie.201108400>.

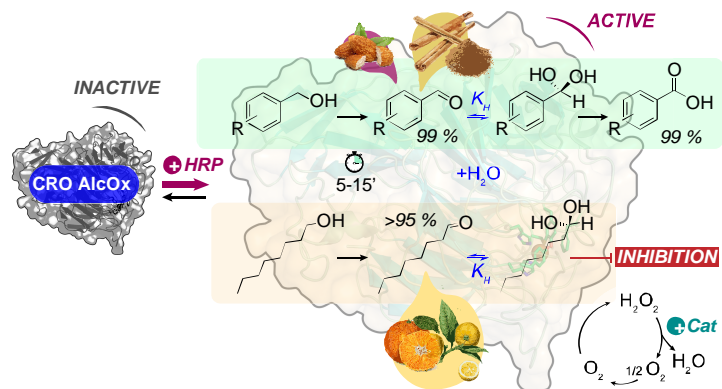
- 621 (57) Borrelli, K. W.; Vitalis, A.; Alcantara, R.; Guallar, V. PELE: Protein Energy Landscape  
622 Exploration. A Novel Monte Carlo Based Technique. *J. Chem. Theory Comput.* **2005**, *1* (6),  
623 1304–1311. <https://doi.org/10.1021/ct0501811>.
- 624 (58) Madadkar-Sobhani, A.; Guallar, V. PELE Web Server: Atomistic Study of Biomolecular  
625 Systems at Your Fingertips. *Nucleic Acids Res* **2013**, *41* (Web Server issue), W322–W328.  
626 <https://doi.org/10.1093/nar/gkt454>.
- 627 (59) Borman, C. D.; Saysell, C. G.; Sokolowski, A.; Twitchett, M. B.; Wright, C.; Sykes, A. G.  
628 Reactivity of Galactose Oxidase. *Coordination Chemistry Reviews* **1999**, *190–192*, 771–  
629 779. [https://doi.org/10.1016/S0010-8545\(99\)00120-4](https://doi.org/10.1016/S0010-8545(99)00120-4).
- 630 (60) Whittaker, J. W. Free Radical Catalysis by Galactose Oxidase. *Chem. Rev.* **2003**, *103* (6),  
631 2347–2364. <https://doi.org/10.1021/cr020425z>.
- 632 (61) Silveira, B. M. P.; Barcelos, M. C. S.; Vespermann, K. A. C.; Pelissari, F. M.; Molina, G.  
633 An Overview of Biotechnological Processes in the Food Industry. In *Bioprocessing for*  
634 *Biomolecules Production*; John Wiley & Sons, Ltd, **2019**; pp 1–19.  
635 <https://doi.org/10.1002/9781119434436.ch1>.
- 636 (62) Pessôa, M. G.; Paulino, B. N.; Molina, G.; Pastore, G. M. Prospective Research and Current  
637 Technologies for Bioflavor Production. In *Bioprocessing for Biomolecules Production*;  
638 John Wiley & Sons, Ltd, **2019**; pp 93–123. <https://doi.org/10.1002/9781119434436.ch5>.
- 639 (63) Humphreys, K. J.; Mirica, L. M.; Wang, Y.; Klinman, J. P. Galactose Oxidase as a Model  
640 for Reactivity at a Copper Superoxide Center. *J. Am. Chem. Soc.* **2009**, *131* (13), 4657–  
641 4663. <https://doi.org/10.1021/ja807963e>.
- 642 (64) Whittaker, M. M.; Whittaker, J. W. The Active Site of Galactose Oxidase. *J. Biol. Chem.*  
643 **1988**, *263* (13), 6074–6080.
- 644 (65) Hartmans, S.; de Vries, H. T.; Beijer, P.; Brady, R. L.; Hofbauer, M.; Haandrikman, A. J.  
645 Production of Oxidized Guar Galactomannan and Its Applications in the Paper Industry. In  
646 *Hemicelluloses: Science and Technology*; ACS Symposium Series; American Chemical  
647 Society, **2003**; Vol. 864, pp 360–371. <https://doi.org/10.1021/bk-2004-0864.ch023>.
- 648 (66) Saysell, C. G.; Borman, C. D.; Baron, A. J.; McPherson, M. J.; Sykes, A. G. Kinetic Studies  
649 on the Redox Interconversion of GOase<sub>semi</sub> and GOase<sub>ox</sub> Forms of Galactose Oxidase with  
650 Inorganic Complexes as Redox Partners. *Inorg. Chem.* **1997**, *36* (20), 4520–4525.  
651 <https://doi.org/10.1021/ic970255m>.
- 652 (67) Kurek, B.; Kersten, P. J. Physiological Regulation of Glyoxal Oxidase from *Phanerochaete*  
653 *chrysosporium* by Peroxidase Systems. *Enzyme and Microbial Technology* **1995**, *17* (8),  
654 751–756. [https://doi.org/10.1016/0141-0229\(95\)00003-N](https://doi.org/10.1016/0141-0229(95)00003-N).
- 655 (68) Daou, M.; Faulds, C. B. Glyoxal Oxidases: Their Nature and Properties. *World J Microbiol*  
656 *Biotechnol* **2017**, *33* (5), 87. <https://doi.org/10.1007/s11274-017-2254-1>.
- 657 (69) Daou, M.; Piumi, F.; Cullen, D.; Record, E.; Faulds, C. B. Heterologous Production and  
658 Characterization of Two Glyoxal Oxidases from *Pycnoporus cinnabarinus*. *Appl. Environ.*  
659 *Microbiol.* **2016**, *82* (16), 4867–4875. <https://doi.org/10.1128/AEM.00304-16>.
- 660 (70) Marteau, C.; Ruyffelaere, F.; Aubry, J.-M.; Penverne, C.; Favier, D.; Nardello-Rataj, V.  
661 Oxidative Degradation of Fragrant Aldehydes. Autoxidation by Molecular Oxygen.  
662 *Tetrahedron* **2013**, *69* (10), 2268–2275. <https://doi.org/10.1016/j.tet.2013.01.034>.
- 663 (71) Sankar, M.; Nowicka, E.; Carter, E.; Murphy, D. M.; Knight, D. W.; Bethell, D.; Hutchings,  
664 G. J. The Benzaldehyde Oxidation Paradox Explained by the Interception of Peroxy Radical  
665 by Benzyl Alcohol. *Nature Communications* **2014**, *5*, 3332.  
666 <https://doi.org/10.1038/ncomms4332>.

- 667 (72) Andberg, M.; Mollerup, F.; Parikka, K.; Koutaniemi, S.; Boer, H.; Juvonen, M.; Master, E.;  
668 Tenkanen, M.; Kruus, K. A Novel *Colletotrichum graminicola* Raffinose Oxidase in the  
669 AA5 Family. *Applied and Environmental Microbiology* **2017**, *83* (20).  
670 <https://doi.org/10.1128/AEM.01383-17>.
- 671 (73) Mollerup, F.; Aumala, V.; Parikka, K.; Mathieu, Y.; Brumer, H.; Tenkanen, M.; Master, E.  
672 A Family AA5\_2 Carbohydrate Oxidase from *Penicillium rubens* Displays Functional  
673 Overlap across the AA5 Family. *PLOS ONE* **2019**, *14* (5), e0216546.  
674 <https://doi.org/10.1371/journal.pone.0216546>.
- 675 (74) Bechi, B.; Herter, S.; McKenna, S.; Riley, C.; Leimkühler, S.; Turner, N. J.; Carnell, A. J.  
676 Catalytic Bio–Chemo and Bio–Bio Tandem Oxidation Reactions for Amide and Carboxylic  
677 Acid Synthesis. *Green Chem.* **2014**, *16* (10), 4524–4529.  
678 <https://doi.org/10.1039/C4GC01321B>.  
679  
680



681 **FOR TABLE OF CONTENTS USE ONLY**

682



683

684

685

686

687 **SYNOPSIS**

688 Establishing Copper-Radical Oxidases as promising biocatalysts for the sustainable production of

689 natural aliphatic aldehydes for flavors and fragrances industry.